Nano Energy 65 (2019) 103956

Contents lists available at ScienceDirect

Nano Energy

journal homepage: www.elsevier.com/locate/nanoen

Full paper

Electron transfer in nano-scale contact electrification: Atmosphere effect on the surface states of dielectrics

Shiquan Lin[a,b], Liang Xu[a,b], Wei Tang[a,b], Xiangyu Chen[a,b], Zhong Lin Wang[a,b,c,*]

[a] Beijing Institute of Nanoenergy and Nanosystems, Chinese Academy of Sciences, Beijing, 100083, PR China
[b] School of Nanoscience and Technology, University of Chinese Academy of Sciences, Beijing, 100049, PR China
[c] School of Materials Science and Engineering, Georgia Institute of Technology, Atlanta, GA, 30332-0245, USA

ARTICLE INFO

Keywords:
Contact electrification
Electron transfer
Atmosphere effect
Oxygen
Surface states measurement

ABSTRACT

Contact electrification (CE) is a common phenomenon, in which the identity of the charge carriers has been debated for decades. Recently, the temperature and photoexcitation effects in CE reveal that the electron in the surface states of dielectrics is the charge carriers, which are responsible for the creation of electrostatic charges. Therefore, the electron transfer in CE may be predicted and controlled by measuring and changing the surface states of dielectrics. Here, a new method to measure the surface states of dielectric based on bias effect in CE is proposed. The CE between metals and dielectrics is performed in different atmospheres, and the surface state density (SSD) and highest occupied surface state level (HOSL) of the dielectric are measured by the method. The results suggest that both the SSD and HOSL of the dielectric can be changed by the adsorption of gas molecules. Particularly, the O_2 molecule is found to shift the HOSL of the dielectric to a lower energy level and make the dielectric more likely to be negatively charged. The findings provide a method to control charge transfer characteristics in CE by changing the O_2 concentration in the atmosphere, and the surface states measurement method has implications for the characterization of the CE properties of materials.

1. Introduction

Contact electrification (CE) (or triboelectrification) is a common phenomenon in our daily life, which has been known for more than 2600 years. In the past, CE was usually regarded as an 'unpredictable' phenomenon [1] and the method to control contact charge transfer was limited, because the mechanism of the CE was ambiguous and the identity of charge carriers in CE was not clear when the dielectric is involved in the CE [2–4]. Recently, the mechanism of CE become a hot topic owing to the invention of triboelectric nanogenerators (TENGs), which are used to convert ubiquitous ambient mechanical energy into electricity based on CE [5–8]. The latest studies, such as the temperature effect [9,10] and the photon excitation effect [11] in CE, revealed that the electron trapped in the surface states of dielectrics is the charge carrier in CE between metals and dielectrics. According to the surface state theory, the electron transfer can be accurately predicted if the surface states (surface state density, SSD and highest occupied surface state level, HOSL) of the dielectric and the Fermi level of the metal are known [12]. Also, the electron transfer can be controlled by changing the surface states of the dielectric, which mainly result from the surface dangling bonds, lattice imperfections and adsorbed molecules [13]. Here, the number and identity of adsorbed molecules on the material surfaces highly depend on the atmosphere. It implies that the surface states and CE properties of dielectrics can be controlled by performing the CE in different atmospheres.

In fact, the atmosphere has been demonstrated to affect the CE significantly in macro-scale. The charge transfer between two solids was found to be very different in different gas pressures and different pure gas (Such as O_2, N_2, Ar et al.) atmospheres [14]. Also, it was found that the transferred charge density in CE will increase when the newly created surfaces are exposed to the atmosphere [15]. In particular, some gas molecules, such as O_2 molecules, can even reverse the polarity of transferred charges in CE [16]. Based on the effect of atmosphere on the CE, a gas-enhanced TENG was designed for energy harvesting [17]. However, the mechanism of the atmosphere effect in CE hasn't been clearly explained yet. Though the adsorption of gas molecules and changing of the surface states of dielectrics were both suspected to be responsible for the atmosphere effect in CE [15], it still lacks direct evidences for the changing of the surface states of dielectrics induced by adsorbed gas molecules. And the measurement of surface states of dielectrics in various atmosphere conditions still remains challenging.

In this study, the CE between metals and dielectrics was performed

* Corresponding author. Beijing Institute of Nanoenergy and Nanosystems, Chinese Academy of Sciences, Beijing, 100083, PR China.
E-mail address: zlwang@binn.cas.cn (Z.L. Wang).

https://doi.org/10.1016/j.nanoen.2019.103956
Received 1 July 2019; Received in revised form 24 July 2019; Accepted 30 July 2019
Available online 08 August 2019

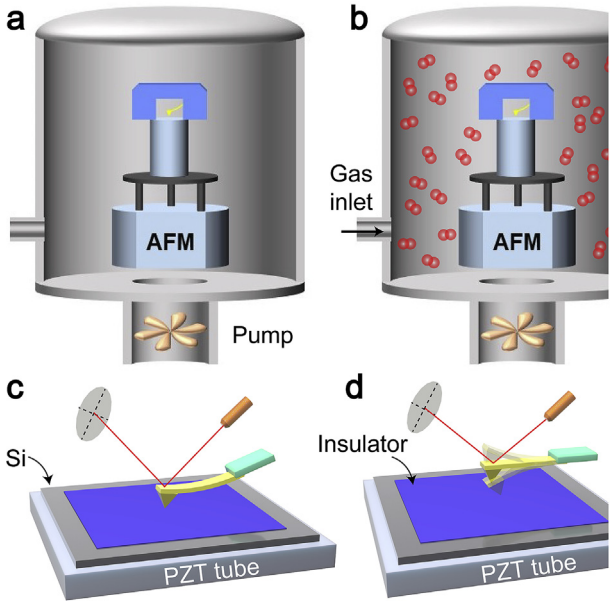

Fig. 1. Schematic illustration of the AFM experiments in the vacuum chamber. (a) Schematics of the vacuum AFM. (b) Pure gas (O_2, N_2 or Ar) is refilled into the chamber. (c) The generation of the triboelectric charge on the dielectric surface by using contact mode. (d) The measurement of the transferred charge density on the dielectric surface by using KPFM mode.

in different atmosphere conditions at nano-scale by using atomic force microscopy (AFM) and Kelvin probe force microscopy (KPFM) [18–20]. The effect of adsorption of different gas molecules on the CE was discussed. Further, a method to measure the surface states of dielectrics based on KPFM was proposed, and the effect of atmosphere on the surface states of dielectrics was studied. It was found that the adsorbed O_2 molecules can shift the HOSL of dielectrics and change the electron transfer in CE. Based on the experiment results, an electron transfer model was proposed to explain the effect of atmosphere on the CE.

2. Results and discussion

In order to control the atmosphere in CE, the AFM equipment was installed into a vacuum chamber, as shown in Fig. 1a. The gas pressure in the chamber can be controlled from 1×10^{-3} Pa–1×10^{5} Pa. As shown in Fig. 1b, pure gases (O_2, N_2 and Ar) can be refilled into the vacuum chamber when the chamber pressure is pumped to 1 Pa, which can be achieved by using a mechanical pump. So that the CE can be performed in different pure gas atmosphere conditions by using our vacuum AFM equipment. Here, ceramic thin films (SiO_2 and AlN; 100 nm thick) and polymer thin films (polyvinyl chloride, PVA and polymethyl methacrylate, PMMA; 500 nm thick) deposited on heavily doped silicon wafers were used as dielectric samples. The metal contact side was a Pt/Ir coated silicon tip, which has good wear-resisting performance. As shown in Fig. 1c, the triboelectric charge on the dielectric surfaces was generated by rubbing with the tip in contact mode, and the contact force was set to be ~5 nN. The triboelectric charge density on the dielectric surface was measured by using FM (frequency modulation) -KPFM mode after the CE, as shown in Fig. 1d. In order to exclude the influence of the tip wear on the CE, the wear resistance of the tip was tested. Fig. S1a (Supporting Information) gives the initial tip topography, and Fig. S1b gives the tip topography after rubbing the SiO_2 surface in contact mode for 30 min. There was no visible tip damage observed in the scanning electron microscopy (SEM) images.

In previous studies in macro-scale, the triboelectric charge density was easy to reach the threshold of gas breakdown, which made the atmosphere effect in CE complicated [21,22]. Fortunately, it has been demonstrated that the threshold of the dielectric surface charge density to induce gas breakdown will get larger when the thickness of the dielectric film on the conductive electrode get smaller [23]. In our AFM experiments at nano-scale, the thickness of the dielectric layer on the conductive electrode was only a few hundred nanometers. For this thickness, the threshold of the surface charge density to induce gas breakdown will be a few thousand microcoulombs per square meter according to previous studies (more than 3000 μCm^{-2} for 100 nm thick; more than 1000 μCm^{-2} for 500 nm thick) [23]. Hence, the gas breakdown is hard to be induced in our experiments, since that the triboelectric charge density generated in CE is generally less than 1000 μCm^{-}

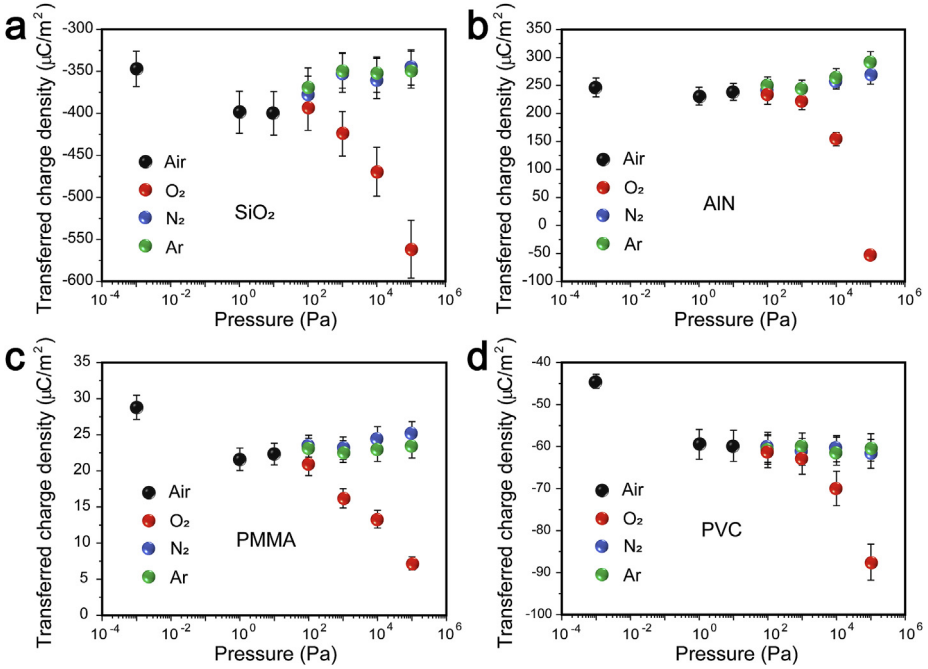

Fig. 2. The CE between Pt/Ir coated tip and dielectric surfaces in different atmosphere conditions. The transferred charge density on the (a) SiO_2, (b) AlN, (c) PMMA and (d) PVC surfaces induced by contacting with the tip in O_2, N_2, Ar and air atmospheres at different gas pressures.

[2].

In the experiments, the air pressures changed from 1×10^{-3} Pa–10 Pa, and the pure gas pressures (O_2, N_2 and Ar) changed from 1×10^2 Pa to 1×10^5 Pa, because it is hard to control the refilled pure gas pressure when the pressure is less than 1×10^2 Pa in the vacuum chamber. Fig. 2 gives the transferred charge density on the dielectric surfaces after being contacted by the Pt/Ir coated tip in O_2, N_2, Ar and air atmospheres at different gas pressures. (The surface potential of the dielectrics after CE in different atmospheres are shown in Fig. S2, Supporting Information). In Fig. 2, it can be seen that the triboelectric charge on all the dielectric surfaces used in our experiments became more negative when the air pressure changed from 1×10^{-3} Pa–10 Pa. When the O_2 was refilled into the chamber, the transferred charge on the dielectric surfaces went negative more significantly. The negative charge density on the SiO_2 and PVC surfaces increased, and the positive charge density on the PMMA surface decreased with the increase of O_2 gas pressure. In particular, the transferred charges on the AlN surface were positive before the O_2 was refilled into the chamber, and the positive charge density decreased when the O_2 gas pressure increased. When the O_2 gas pressure reached to 1×10^5 Pa, the transferred charge polarity on the AlN surface reversed from positive to negative. This phenomenon is consistent with previous studies in macro-scale, in which the reversal of the transferred charge polarity (changing from positive to negative) caused by O_2 was also observed in CE [16]. Based on the experiment results, the O_2 in the air might also play a key role in the effect of air pressure on the CE, because that the transferred charge on the dielectric surfaces also became more negative when the air pressure increased from 1×10^{-3} Pa–10 Pa, which was consistent with the effect of O_2 on the CE.

The effects of N_2 and Ar on the CE were not significant as shown in Fig. 2. The transferred charge density on the dielectric surfaces remained nearly constant when the N_2 and Ar pressures changed from 1×10^2 Pa to 1×10^5 Pa. It needs to be mentioned that the transferred charge density on the SiO_2 and AlN surfaces in the N_2 and Ar atmospheres was approximately the same to that in 1×10^{-3} Pa vacuum, as shown in Fig. 2a and b; while the transferred charge density on the PMMA and PVC surfaces was more negative in the N_2 and Ar atmospheres comparing to that in the 1×10^{-3} Pa vacuum condition, as shown in Fig. 2c and d. The effect of the adsorption of O_2 molecules on the CE might be responsible for these results. In the 1×10^{-3} Pa vacuum condition, the O_2 molecules desorbed from the dielectric surfaces, and the dielectrics showed their 'intrinsic' CE properties. When the air pressure rose up to 1 Pa before the N_2 or Ar was refilled, the O_2 molecules adsorbed on the dielectric surfaces and made them tending to be negatively charged. For SiO_2 and AlN, the N_2 molecules and Ar molecules replaced the O_2 molecules on the surfaces, when N_2 or Ar was refilled into the chamber. Without the effect of O_2 molecules, the transferred charge on the SiO_2 and AlN surfaces maintains similar situation as in 1×10^{-3} Pa vacuum. For PMMA and PVC, the O_2 molecules might adsorb too tight to be replaced by N_2 and Ar on the surfaces, and the transferred charge density on the surfaces remained approximately equal to the charge density generated in the 1 Pa vacuum condition.

The results suggest that N_2 and Ar cannot change the CE properties of dielectrics significantly, while the adsorption of O_2 can make dielectrics more likely to be negatively charged in CE. However, it is still under debate that whether the O_2 effect is caused by physical adoption or chemical adsorption (oxidation). And how the adoption of O_2 affects the surface states of dielectrics still remains poorly understood.

The manner (physical or chemical) of the O_2 molecules adsorbing on the dielectric surfaces in CE is discussed here, as shown in Fig. 3. The CE between the dielectric and the tip was performed in 1×10^5 Pa O_2 atmosphere first (The charging area is 5 μm × 5 μm). Then, the gas pressure in the chamber was pumped to 1×10^{-3} Pa, and the dielectric was rubbed by the tip again (The charging area is 2 μm × 2 μm in the center of the test area). The SiO_2 and AlN were negatively charged in the 1×10^5 Pa O_2 atmosphere, which means that the electrons transferred from the tip to the sample surfaces in this case. When the gas pressure decreased to 1×10^{-3} Pa, the electrons transferred backed to the tip in the CE, and the surface potential of the charging area (2 μm × 2 μm) became more positive, as shown in Fig. 3a, b and c. It indicates that the phenomenon of CE property changing induced by O_2 adsorption on SiO_2 and AlN surfaces is reversible, and O_2 should be physically adsorbed on the SiO_2 and AlN surfaces in CE. In the 1×10^5 Pa O_2 atmosphere, the O_2 molecules physically adsorbed on the SiO_2 and AlN surfaces, and made them very negatively charged in CE. When the gas pressure was pumped to 1×10^{-3} Pa, the O_2 molecules desorbed from the surface, and the SiO_2 and AlN showed their 'intrinsic' CE properties. In this case, the electrons would transfer back to the tip since that the 'intrinsic' SiO_2 and AlN could not be so negatively charged as shown in Fig. 2a and b.

Different with SiO_2 and AlN, the electrons would not transfer back once they have been generated on the PVA and PMMA surfaces in 1×10^5 Pa O_2 atmosphere, as shown in Fig. 3d, e and f. It suggests that the effect of O_2 adsorption on the CE properties of PVC and PMMA is permanent, and O_2 should be chemically adsorbed (oxidation) on the PVC and PMMA surfaces. The chemical bonds between O atoms and PVC or PMMA were too tight to be broken, though the gas pressure was pumped to 1×10^{-3} Pa. And the PVC and PMMA would no longer show their 'intrinsic' CE properties once the O atoms were bonded to the PVC and PMMA in the CE. Hence, the results show that the manner of O_2 adsorption in CE depends on the dielectric properties, and both physical and chemical adsorption of O_2 on the dielectric can make the dielectric more negatively charged in CE.

Actually, both physical and chemical adsorption of gas molecules on the dielectric surfaces are suspected to affect the surface states of dielectrics significantly, and thus change the CE properties of dielectrics. In order to verify this hypothesis, a method to measure the surface states (SSD and HOSL) of dielectrics was proposed based on previous studies about the bias effect in the CE [24]. As shown in Fig. 4a, we assume that the Fermi level of the metal is lower than the HOSL of the dielectric. In this case, the electrons will transfer from the dielectric to the metal. When a negative bias is applied to the tip, the effective Fermi level of the metal will rise up and the number of electrons transferred from the dielectric to the metal will decrease, as shown in Fig. 4b. If the negative bias is high enough, the effective Fermi level of the metal will be equal to the HOSL of the dielectric (Fig. 4c), or even higher than the HOSL of the dielectric, and electrons will transfer from the metal to the dielectric (Fig. 4d). According to previous studies about the bias effect in the CE, the change of the effective Fermi level of the metal can be expressed with following equations (The variables are shown in Fig. 4e) [24]:

$$\Delta E_f = \sigma_1 z e/\varepsilon_0 \tag{1}$$

and

$$\sigma + \sigma_1 + \sigma_2 = 0 \tag{2}$$

where ΔE_f denotes the change of the effective Fermi level of the metal (tip), σ_1 denotes the charge density on the metal (tip) surface induced by the triboelectric charge on the dielectric surface, z denotes the tunneling distance of the electrons in CE, e denotes the electron charge, ε_0 denotes the vacuum dielectric constant, σ_2 denotes the induced charge density on the Si surface, and σ denotes the transferred charge density on dielectric surface.

According to the Poisson equation, the bias V_t between the metal (tip) and the dielectric substrate (Si) can be written as below:

$$V_t = \frac{\sigma_1}{\varepsilon_0} z - \frac{\sigma_2}{\varepsilon \varepsilon_0} t \tag{3}$$

where t denotes the thickness of the dielectric and ε denotes the relative dielectric constant of the dielectric.

Considering that the electron tunneling distance is much smaller

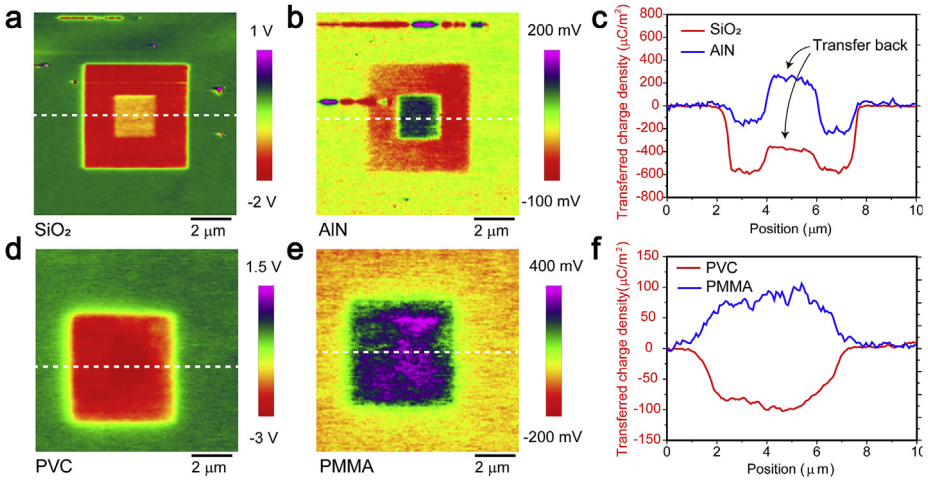

Fig. 3. The adsorption test of O_2 on the dielectric surfaces in CE. The surface potential of (a) SiO_2, (b) AlN, (d) PVC and (e) PMMA after they are contacted by the tip in 1×10^5 Pa O_2 (5 μm × 5 μm) and 1×10^{-3} Pa vacuum (2 μm × 2 μm) atmospheres in sequence. (c) The profile of transferred charge density on the SiO_2 and AlN surfaces extracted from the white dotted lines in (a) and (b). (f) The profile of transferred charge density on the PVC and PMMA surfaces extracted from the white dotted lines in (d) and (e).

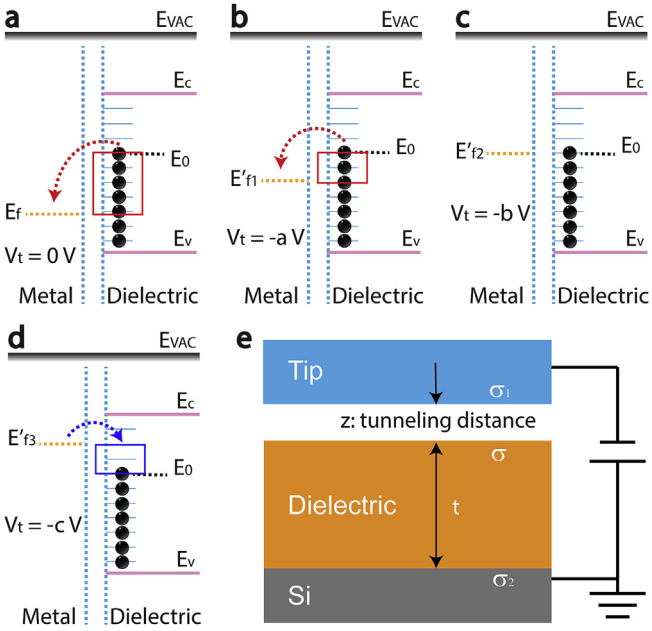

Fig. 4. Schematics of the bias effect on the CE and the method the measure the surface states of dielectrics. The charge transfer between the metal and the dielectric, when (a) 0 V, (b) -a V, (c) -b V and (d) -c V bias are applied to the metal ($0 < a < b < c$). (e) Illustration of the CE between the tip and the dielectric in our experiments. (E_c is the bottom of the conductive band of the dielectric, E_v is the top of the valence band).

than the thickness of the dielectric layer, Equation (3) can be expressed as following:

$$V_t \approx -\frac{\sigma_2}{\varepsilon\varepsilon_0} t \tag{4}$$

Combining Equations (1), (2) and (4), the effect of tip bias on the change of tip effective Fermi level can be described as:

$$\Delta E_f = \left(\frac{V_t \varepsilon\varepsilon_0}{t} - \sigma\right) ze/\varepsilon_0 \tag{5}$$

According to the surface state theory [12], the transferred charge density on the dielectric surfaces when they contact the metal can be expressed as following:

$$\sigma = e \int_{E_0}^{E_f} N(E) dE \tag{6}$$

where E_0 denotes the HOSL of the dielectric, E_f denotes the effective Fermi level of the tip, and $N(E)$ denotes the SSD of the dielectric at energy level E.

The SSD of the dielectric can be calculated by the following equation through derivation of Equation (6):

$$\sigma'(E_f) = eN(E_f) \tag{7}$$

According to Equation (5), the effective Fermi level of the tip can be controlled by applying a bias to the tip, which will induce a variation in the transferred charge density. Hence, the relation between the transferred charge density on the dielectric surface and the effective Fermi level of the tip can be obtained by performing the CE when different biases are applied between the tip and the substrate. And then, the SSD of the dielectric can be obtained by calculating the derivative of the transferred charge density on the dielectric surface with respect to the effective Fermi level of the tip according to Equation (7). Moreover, the HOSL of the dielectric is equal to the effective Fermi level of the tip, which can make no electron transfer between the tip and the dielectric.

Based on the above equations, the CE between the tip and the dielectric was performed when different biases were applied, and the surface states of the dielectric in different atmospheres were calculated. As shown in Fig. 5a, the tip was controlled to rub the SiO_2 surface line-by-line, and the tip bias varied from -10 V to $+10$ V uniformly in $+1$ V intervals. It is obvious that the negative tip bias made the SiO_2 tending to be negatively charged and the positive tip bias made SiO_2 tending to be positively charged. And there was a tip bias where no electron transferred between the tip and SiO_2, is pointed out by the black arrows in Fig. 5a (It can be called as a 'cut-off' bias). Interestingly, the 'cut-off' bias in CE between the tip and SiO_2 was most positive in 1×10^5 Pa O_2 comparing to that in 1×10^5 Pa N_2, 1×10^5 Pa Ar and 1×10^{-3} Pa vacuum. It means that the HOSL of the SiO_2 is lowest in 1×10^5 Pa O_2 atmosphere, and indicates that the O_2 molecules on the SiO_2 surface can shift the HOSL of the SiO_2 to a lower energy level. In order to calculate the shift of the HOSL and the change of SSD induced by adsorption of gas molecules, the relation between the transferred charge density on the SiO_2 surface and the tip bias was extracted from Fig. 5a (white dotted line), as shown in Fig. 5b and c. It can be seen that the transferred charge density changed almost linearly with the tip bias. The 'cut-off' bias in different atmospheres are also shown in Fig. 5b and c (The 'cut-off' biases were 0.5 V in 1×10^{-3} Pa vacuum, 2.8 V in $1 \times$

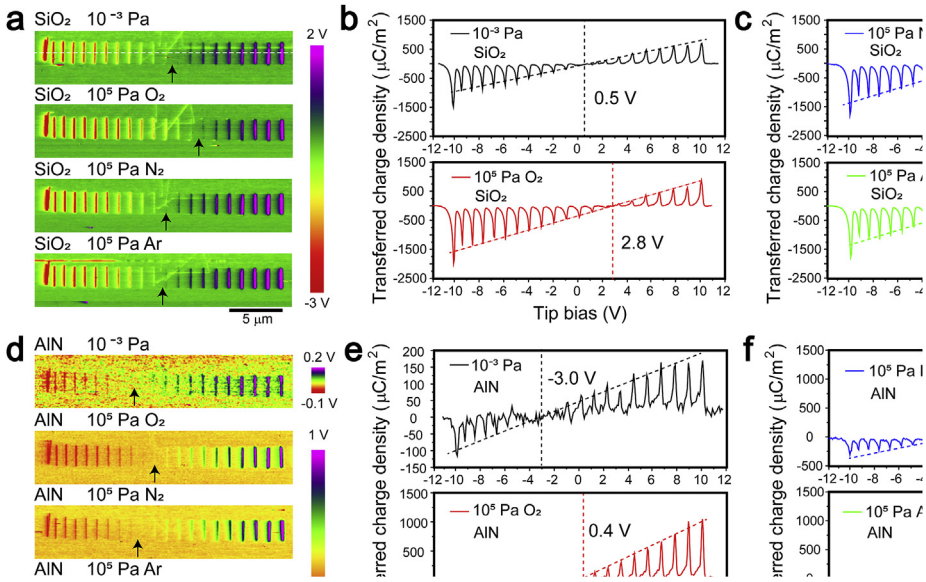

Fig. 5. Measurement of the surface states of SiO_2 and AlN in different atmospheres. The surface potential of (a) SiO_2, (d) AlN surfaces when they are rubbed by the tip line-by-line in different atmospheres, and the tip bias varied from −10 V to +10 V uniformly in +1 V intervals. The relation between the tip bias and the transferred charge density on (b, c) SiO_2 and (e, f) AlN surfaces in different atmospheres.

10^5 Pa O_2, 0.4 V in 1×10^5 Pa N_2 and 0.6 V in 1×10^5 Pa Ar). Here, the relation between the transferred charge density on the SiO_2 surface and the tip bias can be expressed as following:

$$\sigma = \alpha(V_t - \beta) \tag{8}$$

where α denotes the slope of the relation between the transferred charge density and the tip bias, and β denotes the 'cut-off' bias.

Combining Equations (5) and (8), the relation between the transferred charge density on the SiO_2 surface and the effective Fermi level of the tip can be expressed as following:

$$E_f = E_{Pt/Ir} + \Delta E_f = E_{Pt/Ir} + \left(\sigma\left(\frac{\varepsilon\varepsilon_0}{\alpha t} - 1\right) + \frac{\beta\varepsilon\varepsilon_0}{t}\right)ze/\varepsilon_0 \tag{9}$$

where $E_{Pt/Ir}$ denotes the 'intrinsic' Fermi level of the Pt/Ir coated tip. Here, the parameter l is used to replace $\frac{\varepsilon\varepsilon_0}{\alpha t} - 1$, m is used to replace $\frac{\beta\varepsilon\varepsilon_0}{t}$, and k is used to replace ze/ε_0, then:

$$E_f = E_{Pt/Ir} + (\sigma l + m)k \tag{10}$$

Combining Equations (7) and (10), the SSD can be calculated as following:

$$N(E_f) = 1/lke \tag{11}$$

The HOSL of the SiO_2 is equal to the effective Fermi level of the tip, which makes no electrons transfer between the tip and SiO_2. Hence, the HOSL of the SiO_2 can be calculated as following according to Equation (10):

$$E_0 = E_{Pt/Ir} + mk \tag{12}$$

In 1×10^{-3} Pa vacuum, the α and β were fitted to be 90 $\mu Cm^{-2}V^{-1}$ and 0.5 V respectively, as shown in Fig. 5b. Therefore, $l = 2.835$ and $m = 172.6\mu Cm^{-2}$. And the parameter k was calibrated to be -1.76×10^{-4} $eVm^2\mu C^{-1}$ by using a reference Au coated tip with a different 'intrinsic' Fermi level to measure the surface states of SiO_2 in 1×10^{-3} Pa vacuum (The calibration is shown in Supporting Information, Fig. S3). According to Equation (11), the average SSD of SiO_2 in 1×10^{-3} Pa vacuum was calculated to be 2.00×10^{12} $eV^{-1}cm^{-2}$.

Here, we defined the vacuum energy level as 0 eV, and the 'intrinsic' Fermi level of the Pt/Ir coated tip was calibrated to be −5.185 eV by measuring the contact potential difference (CPD) between the Pt/Ir coated tip and Au coated tip (The calibration is shown in Supporting Information). According to Equation (12), the HOSL of SiO_2 in 1×10^{-3} Pa vacuum is calculated to be −5.215 eV.

Further, the average SSDs of the SiO_2 in 1×10^5 Pa O_2, 1×10^5 Pa N_2 and 1×10^5 Pa Ar atmospheres were calculated to be 3.22×10^{12} $eV^{-1}cm^{-2}$, 3.63×10^{12} $eV^{-1}cm^{-2}$ and 3.13×10^{12} $eV^{-1}cm^{-2}$, respectively. And the HOSL of the SiO_2 in 1×10^5 Pa O_2, 1×10^5 Pa N_2 and 1×10^5 Pa Ar atmospheres were calculated to be −5.355 eV, −5.209 eV and −5.221 eV, respectively (The effect of the gas adsorption on the Fermi level of Pt/Ir tip was not considered here, since the metal is an 'ocean' of electrons, and the Fermi level of the metal is hard to be shifted by the gas adsorption). It can be seen that both the SSD and HOSL of the SiO_2 can be affected by the adsorbed gas molecules (O_2, N_2 and Ar). The SSD of the SiO_2 increased when the gas molecules adsorbed on the surface. And the HOSL of the SiO_2 could be shifted by −0.17 eV, when the O_2 molecules adsorbed on the surface in 1×10^5 Pa O_2 atmosphere. The negative shift of the HOSL of SiO_2 made the SiO_2 more likely to be negatively charged, so the negative charge density on the SiO_2 surface increased with the increase of the O_2 pressure.

For AlN, the 'cut-off' bias was 0.4 V in 1×10^5 Pa O_2, which was also most positive comparing to that in other atmospheres (−3.0 V in 1×10^{-3} Pa vacuum, −2.1 V in 1×10^5 Pa N_2 and -2.6 V in 1×10^5 Pa Ar), as shown in Fig. 5d, e and f. According to the 'cut-off' bias, the HOSL of AlN in 1×10^{-3} Pa vacuum, 1×10^5 Pa O_2, 1×10^5 Pa N_2 and 1×10^5 Pa Ar atmospheres were calculated to be −4.774 eV, −5.240 eV, −4.8971 eV and −4.8286 eV, respectively. It worth to be pointed out that the HOSL of AlN in 1×10^{-3} Pa vacuum was higher than the Fermi level of the Pt/Ir coated tip, and the AlN was positively charged in the CE. When the O_2 molecules adsorbed on the AlN surface in 1×10^5 Pa O_2 atmosphere, the HOSL of the AlN was shifted to be −5.240 eV, which was lower than the Fermi level of Pt/Ir coated tip, and the polarity of the transferred charge on the AlN surface was reversed to be negative. From Fig. 5e and f, the SSD of AlN in high energy level was higher than that in low energy level. In CE, the SSD near the HOSL can affect the CE most significantly. Hence, the SSDs of the AlN near the HOSL in 1×10^{-3} Pa vacuum, 1×10^5 Pa O_2, 1×10^5 Pa N_2 and 1×10^5 Pa Ar atmospheres were calculated to be 0.11×10^{12} $eV^{-1}cm^{-2}$, 0.30×10^{12} $eV^{-1}cm^{-2}$, 0.42×10^{12} $eV^{-1}cm^{-2}$ and 0.39×10^{12} $eV^{-1}cm^{-2}$, respectively. It can be seen that the atmosphere can affect both the SSD and HOSL of the AlN, and the O_2 molecules can also shift the HOSL of AlN to a lower energy level. Using the same method, the surface states of PMMA and PVC were measured as shown in Fig. S4 (Supporting Information). The shift of the HOSL of PMMA and PVC induced by O_2 chemical adsorption was also observed in Fig. S4.

The calculations and analyses suggest that the adsorption of O_2, N_2 and Ar, can increase the SSD of the dielectrics. However, only O_2 can shift the HOSL of the dielectrics to a lower energy level and make the

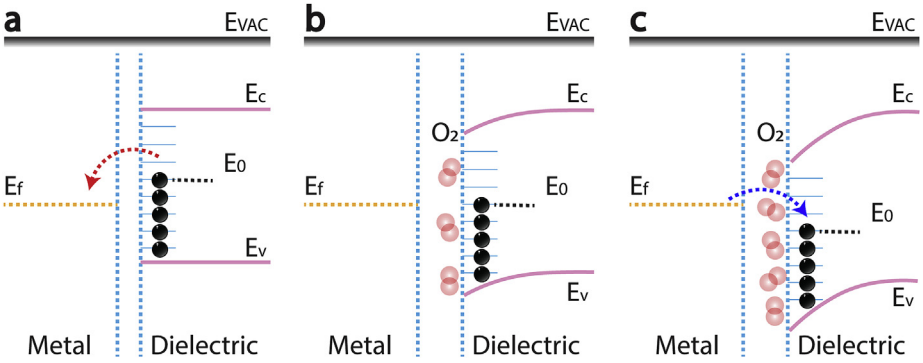

Fig. 6. The band structure model of the O_2 effect on the CE between the metal and the dielectric. (a) The CE between the metal and the dielectric without the adsorption of O_2 molecules. (b) The CE between the metal and the dielectric with the adsorption of O_2 molecules on the dielectric surface. (c) The CE between the metal and the dielectric with more O_2 molecules adsorbing on the dielectric surface.

dielectrics more likely to be negatively charged. Here, the band structure model of O_2 effect on the CE between the metal and the dielectric is proposed as shown in Fig. 6. We assume that the 'intrinsic' HOSL of the dielectric is higher than the Fermi level of the metal, and the electrons will transfer from dielectric to the metal in this case (Fig. 6a). When the dielectric is exposed to O_2 atmosphere, the O_2 molecules shift the HOSL of the dielectric to a lower energy level and the charge density on the dielectric surface will become more negative. Particularly, when the HOSL of the dielectric equal to the Fermi level of the metal, there will be no electrons transfer between the metal and the dielectric, as shown in Fig. 6b. If the number of the O_2 molecules on the dielectric surface increase further, the HOSL of the dielectric will be shifted to a lower energy level and the electrons will transfer from the metal to the dielectric surface, and the polarity of the transferred charge in CE will be reversed.

The effect of O_2 molecules on the CE provides a potential method to improve the output performance of the TENG by changing the O_2 concentration in the atmosphere. In addition, the surface states measurement method based on the bias effect in CE may also have implications for the characterization of the CE properties of materials. So far, the best way to describe the CE properties of materials is making the triboelectric series, in which the materials are ranked based on their abilities to gain or lose electrons [25]. However, the SSD and HOSL of the materials, which can determine the number and direction of the transferred electrons in CE, cannot be derived from the triboelectric series. On the contrary, if the SSD and HOSL of the materials are measured, the electrons transfer between the materials can be accurately predicted. In this perspective, the ranking of the SSD and HOSL of the materials may provide more information about the CE properties of materials comparing to the traditional triboelectric series. Hence, the surface states measurement in this paper may provide a new method to calibrate the CE properties of materials.

In conclusion, the CE between a Pt/Ir coated tip and dielectrics was performed in different atmospheres. It was found that the adsorption of O_2 molecules on the surfaces could make the dielectrics more likely to be negatively charged in CE. Further, a method to measure the SSD and HOSL of the dielectrics was proposed and the SSD and HOSL of dielectrics were measure in different atmospheres. The results showed that the adsorption of the gas molecules on the surface can affect both the SSD and HOSL. In particularly, O_2 molecules on the dielectric surface were found to shift the HOSL of the dielectrics to a lower energy level, and made the dielectrics tend to be negatively charged. Finally, the atmosphere effect in the CE was explained clearly by using the surface state theory, in which the electron in the surface states of the dielectric is considered as the charge carrier and the shift of HOSL induced by O_2 molecules is responsible for the atmosphere effect in CE. The findings in this paper provides a potential method to improve the output performance of the TENG by changing the O_2 concentration in the atmosphere. And the surface states measurement method proposed here may provide a new approach to calibrate the CE properties of materials at nano-scale.

3. Experimental section

Sample preparation: The SiO_2 and AlN layer of 100 nm in thickness were deposited on heavily doped silicon wafer by thermal oxidation and magnetron sputtering, respectively. The PVC and PMMA layer of 500 nm in thickness were prepared on the heavily doped silicon wafer by spin coating. The mass fraction of PVA and PMMA solutions used in the spin process were both 2%. The rotational speed used to prepare the polymer films was 2000 r/min.

Vacuum AFM: The commercial AFM/KPFM equipment Multimode 8 (Bruker, USA) was installed into a vacuum chamber. (It should be noted that it is dangerous to put the Multimode 8 into the vacuum chamber directly. In our experiments, the Multimode 8 was modified first. Some components, which cannot withstand negative pressure, have been removed.) The mechanical pump used in the vacuum system is RVP-8 (KYKY Technology, China), and the molecule pump used here is FF160/620F (KYKY Technology, China). The limited vacuum level of the vacuum chamber is 1×10^{-3} Pa.

AFM experiments: The AFM and FM-KPFM experiments were performed by using the home modified vacuum AFM equipment. The Pt/Ir coated silicon tip used here is SCM-PIT (Bruker, USA; coating: Pt/Ir; tip radius: 20 nm; spring constant: 2.8 N/m). In the contact mode scanning, the scan size was set to 5 μm, scan rate was 1 Hz, and the contact force was ~5 nN. The triboelectric charges were detected in FM-KPFM mode, while the peakforce tapping mode was used in main scanning, and the peakforce was set to 200 pN, the lift height was 50 nm and the scan size was 10 μm.

Acknowledgements

Research was supported by the National Key R & D Project from Minister of Science and Technology (2016YFA0202704), Beijing Municipal Science and Technology Commission (Z171100000317001, Z171100002017017, Y3993113DF), National Natural Science Foundation of China (Grant No. 51432005, 51605033, 5151101243, 51561145021).

Appendix A. Supplementary data

Supplementary data to this article can be found online at https://doi.org/10.1016/j.nanoen.2019.103956.

References

[1] D.J. Lacks, Angew. Chem. Int. Ed. 51 (2012) 6822.
[2] J. Wu, X. Wang, H. Li, F. Wang, W. Yang, Y. Hu, Nano Energy 48 (2018) 607.
[3] J.C. Angus, I. Greber, J. Appl. Phys. 123 (2018) 174102.
[4] L.S. McCarty, G.M. Whitesides, Angew. Chem. Int. Ed. 47 (2008) 2188.
[5] F. Fan, Z. Tian, Z.L. Wang, Nano Energy 1 (2012) 328.
[6] G. Zhu, B. Peng, J. Chen, Q. Jing, Z.L. Wang, Nano Energy 14 (2015) 126.
[7] Z.L. Wang, ACS Nano 7 (2013) 9533.
[8] P. Cheng, H. Guo, Z. Wen, C. Zhang, X. Yin, X. Li, D. Liu, W. Song, X. Sun, J. Wang, Z.L. Wang, Nano Energy 57 (2019) 432.

[9] C. Xu, Y. Zi, A.C. Wang, H. Zai, Y. Dai, X. He, P. Wang, Y. Wang, P. Feng, D. Li, Z.L. Wang, Adv. Mater. 30 (2018) 1706790.
[10] S. Lin, L. Xu, C. Xu, A.C. Wang, B. Zhang, P. Lin, Y. Yang, H. Zhao, Z.L. Wang, Adv. Mater. 31 (2019) 1808197.
[11] S. Lin, L. Xu, L. Zhu, X. Chen, Z.L. Wang, Adv. Mater. (2019), https://doi.org/10.1002/adma.201901418.
[12] J. Lowell, A.C. Rose-Innes, Adv. Phys. 29 (1980) 947.
[13] F.A. Vick, Br. J. Appl. Phys. 4 (1953) S1.
[14] K. Han, W. Tang, J. Chen, J. Luo, L. Xu, Z.L. Wang, Adv. Mater. Technol. 4 (2019) 1800569.
[15] J. Lowell, J. Phys. D Appl. Phys. 10 (1977) 65.
[16] J. Chen, W. Tang, C. Lu, L. Xu, Z. Yang, B. Chen, T. Jiang, Z.L. Wang, Appl. Phys. Lett. 110 (2017) 201603.
[17] S. Lv, B. Yu, T. Huang, H. Yu, H. Wang, Q. Zhang, M. Zhu, Nano Energy 55 (2019) 463.
[18] B.D. Terris, J.E. Stern, D. Rugar, H.J. Mamin, Phys. Rev. Lett. 63 (1989) 2669.
[19] S. Lin, T. Shao, Phys. Chem. Chem. Phys. 19 (2017) 29418.
[20] C. Schonenberger, S.F. Alvarado, Phys. Rev. Lett. 65 (1990) 3162.
[21] B.A. Kwetkus, K. Scattler, H. Siegmann, J. Phys. D Appl. Phys. 25 (1992) 139.
[22] J. Wang, C. Wu, Y. Dai, Z. Zhao, A. Wang, T. Zhang, Z.L. Wang, Nat. Commun. 8 (2017) 88.
[23] Y. Zi, C. Wu, W. Ding, Z.L. Wang, Adv. Funct. Mater. 27 (2017) 1700049.
[24] Y. Zhou, S. Wang, Y. Yang, G. Zhu, S. Niu, Z. Lin, Y. Liu, Z.L. Wang, Nano Lett. 14 (2014) 1567.
[25] H. Zou, Y. Zhang, L. Guo, P. Wang, X. He, G. Dai, H. Zheng, C. Chen, A. Wang, C. Xu, Z.L. Wang, Nat. Commun. 10 (2019) 1427.

Dr. Shiquan Lin received his Ph.D. degree from Tsinghua University (THU) in 2018. he now works as a postdoctoral fellow under the supervision of Prof. Zhong Lin Wang in Beijing Institute of Nanoenergy and Nanosystems (BINN), Chinese Academy of Sciences. His research interests include fundamental tribological phenomena, scanning probe microscopy and fist-principle calculation.

Prof. Liang Xu received his Ph.D. degree from Tsinghua University (THU) in 2012, with awards of Excellent Doctoral Dissertation of THU and Excellent Graduate of Beijing. From 2015, he worked as a postdoctoral fellow under the supervision of Prof. Zhong Lin Wang in Beijing Institute of Nanoenergy and Nanosystems (BINN), Chinese Academy of Sciences. He is now an associate professor in BINN. His research interests include triboelectric nanogenerators and self-powered systems, blue energy, fundamental tribological phenomena, scanning probe microscopy and molecular dynamics simulation.

Prof. Wei Tang is an associate professor at the Beijing Institute of Nanoenergy and Nanosystems, Chinese Academy of Sciences. He received his B.S. and Ph.D. degrees from the School of Physics and School of Electronics Engineering and Computer Science in 2008 and 2013, respectively, from Peking University, China. His research interests include triboelectric nanogenerators, self-powered systems and wireless sensing networks, and micro/nanoengineering.

Prof. Xiangyu Chen received his B.S. degree in Electrical Engineering from Tsinghua University in 2007 and his Ph.D. in Electronics Physics from Tokyo Institute of Technology in 2013. Now he is a professor in Beijing Institute of nanoenergy and nanosystems, Chinese Academic of Sciences. His main research interests have been focused on the field of functional dielectric materials, self-powered nano energy system and the nonlinear optical laser system for characterizing the electrical properties of the devices.

Prof. Zhong Lin Wang received his Ph. D from Arizona State University in physics. He now is the Hightower Chair in Materials Science and Engineering, Regents' Professor, Engineering Distinguished Professor and Director, Center for Nanostructure Characterization, at Georgia Tech. Dr. Wang has made original and innovative contributions to the synthesis, discovery, characterization and understanding of fundamental physical properties of oxide nanobelts and nanowires, as well as applications of nanowires in energy sciences, electronics, optoelectronics and biological science. He pioneered the field of piezotronics and piezo-phototronics by introducing piezoelectric potential gated charge transport process in fabricating new electronic and optoelectronic devices.